



# Dynamical symmetry and synchronization in modular networks

To cite this article: H. J. Wang *et al* 2008 *EPL* **81** 60005

View the [article online](#) for updates and enhancements.

## You may also like

- [Non-stationarity and dissipative time crystals: spectral properties and finite-size effects](#)  
Cameron Booker, Berislav Bua and Dieter Jaksch
- [Effect of mixing parts of modular networks on explosive synchronization](#)  
Meng Li, Xin Jiang, Yifang Ma et al.
- [Quantum synchronisation enabled by dynamical symmetries and dissipation](#)  
J Tindall, C Sánchez Muñoz, B Bua et al.

# Dynamical symmetry and synchronization in modular networks

H. J. WANG<sup>1,2</sup>, H. B. HUANG<sup>1(a)</sup>, G. X. QI<sup>1(b)</sup> and L. CHEN<sup>1</sup>
<sup>1</sup> Department of Physics, Southeast University - Nanjing 210096, PRC

<sup>2</sup> Department of Physics, Nanjing Xiaozhuang University - Nanjing 210017, PRC

received 2 October 2007; accepted in final form 22 January 2008

published online 22 February 2008

PACS 05.45.Xt – Synchronization; coupled oscillators

PACS 05.45.Jn – High-dimensional chaos

PACS 89.75.Kd – Patterns

**Abstract** – The effects of dynamical symmetry on the chaotic pattern synchronization in modular networks have been studied. It is found that the topological and the coupling symmetries between modules (subnetworks) can both enhance and speed up the chaotic pattern synchronization between modules. The calculation of Lyapunov exponent shows that this dynamical symmetry is a necessary condition for complete chaotic pattern synchronization in both modular networks composed by identical oscillators and heterogeneous modular networks if the states of nodes are much different from one another.

Copyright © EPLA, 2008

Dynamical synchronization in complex networks has been an interesting research subject in recent years due to its relevance to fields such as ecology [1], neuroscience [2], chemistry [3], laser [4], and plasma [5] etc. For different networks, the global chaotic synchronization has been studied in regular [6], random [7], small-world [8], scale-free [9], and modular [10] networks. Some conclusions on the relations between the network structure and the synchronization are obtained, *e.g.*, random and semi-random (scale free, small-world, etc) networks are more synchronizable than regular networks [6,8]; long-range coupling, age ordering, and weighted distribution of connection strength can enhance the synchronization [7,9].

Another interesting phenomenon is the dynamical pattern (spatiotemporal dynamics) formation in complex networks which usually occurs in heterogeneous networks and in the transition to global synchronization in complex networks [4,5,11] composed by identical oscillators. Many complex networks, *e.g.*, brain and biological networks usually exhibit random (semi-random) topologies with high node connections locally and show some regular topologies globally. This local and global topological structure is just the feature of modular networks [12]. Dynamical pattern formation in a modular network is obviously related to the network functions. Although the pattern formations have been studied in modular

networks [11,12] and the chaotic pattern synchronization (CPS) have been found experimentally in extended systems [4,5], the synchronization between chaotic patterns in networks, however, has not been concerned.

In this letter, we study the CPS between two unidirectionally interlinked modules (a drive module *d* and a response module *r*) with each module intralinked regularly or randomly (see fig. 1). Such a modular network may be a sub-modular network of a hierarchical network [11,12] or a larger complex network. In our present study, the CPS means that the two modules have the same (complete) or similar (phase) spatiotemporal chaotic dynamics. The dynamics of the drive module *d* is described by

$$\dot{\mathbf{x}}_i^d = \mathbf{F}_i^d(\mathbf{x}_i^d) + \sum_j g_{ij}^{dd} \mathbf{H}_{ij}^d(\mathbf{x}_j^d, \mathbf{x}_i^d), \quad (1)$$

and the dynamics of the response module *r* is determined by

$$\dot{\mathbf{x}}_i^r = \mathbf{F}_i^r(\mathbf{x}_i^r) + \sum_j g_{ij}^{rr} \mathbf{H}_{ij}^r(\mathbf{x}_j^r, \mathbf{x}_i^r) + \sum_j g_{ij}^{rd} \mathbf{H}_{ij}^{rd}(\mathbf{x}_j^d, \mathbf{x}_i^r), \quad (2)$$

where  $\dot{\mathbf{x}}_i = \mathbf{F}_i(\mathbf{x}_i)$ ,  $\mathbf{x}_i \in R^{m_i}$ , is the dynamical equation of the isolated node *i*, and it may be different for different node *i* in *d* and *r*. While  $\mathbf{H}_{ij}(\mathbf{x}_j, \mathbf{x}_i) : R^{m_j} \times R^{m_i} \rightarrow R^{m_i}$  and  $g_{ij}$  are the coupling function and the coupling strength from node *j* to node *i*, respectively. The size of the modular networks  $N = N^d + N^r = 2N^d = 2N^r$ . To obtain the CPS between the two modules, we will show that the *topological symmetry*: 1)  $\mathbf{F}_i^d = \mathbf{F}_i^r = \mathbf{F}_i$ , 2)  $\mathbf{H}_{ij}^{dd} = \mathbf{H}_{ij}^{rr} = \mathbf{H}_{ij}^{rd} = \mathbf{H}_{ij}$ ,

(a) E-mail: hongbinh@seu.edu.cn

(b) Present address: Research Center Jülich, Institute of Neurosciences and Biophysics INB-3 - Leo-Brandt-Str., 52425 Jülich, Germany

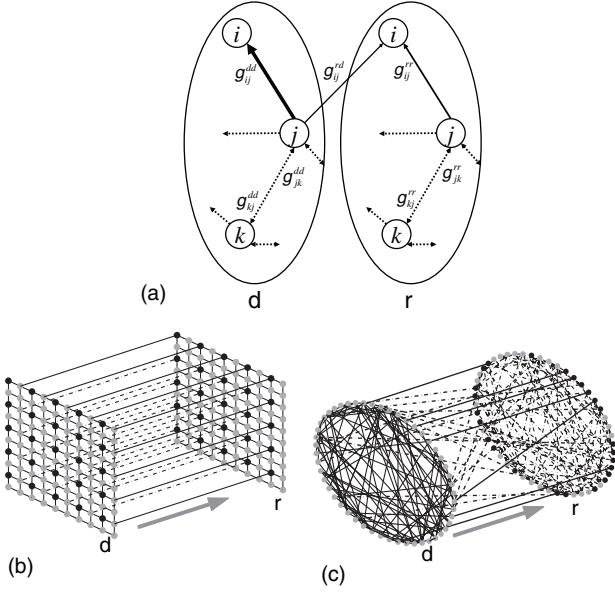


Fig. 1: (a) Schematic illustration of the dynamical symmetry  $g_{ij}^{dd} = g_{ij}^{rd} + g_{ij}^{rr}$  between modules d and r. Module d has the same dynamical topology as module r for  $g_{ij}^{rd} = 0$ . (b) A modular network composed by two interlinked 2D regular lattices with open boundary conditions. Here  $g_{ij}^{dd} = g_{ji}^{dd} = \alpha$ ,  $g_{ij}^{rd} = \beta$ ,  $g_{ij}^{rr} = \alpha - \beta$ , and  $N^d = N^r = 100$ . The black nodes and the gray nodes are in different positions. (c) A random modular network, module d is first generated with probability  $P_1$  and  $g_{ij}^{dd} = g_{ji}^{dd} = \alpha$ , module r is a “copy” of d, thus modules d and r have the same dynamical topology. Then d and r are randomly interlinked with probability  $P_2$ ,  $g_{ij}^{rd} = \beta$ , and  $g_{ij}^{rr} = \alpha - \beta$ .

and the coupling symmetry: 3)  $g_{ij}^{dd} = g_{ij}^{rd} + g_{ij}^{rr}$  (see fig. 1a),  $\forall i$  should exist, that is, modules d and r have the same dynamical topology for  $g_{ij}^{rd} = 0$ . If module d (r) is heterogeneous, i.e., modular d (r) is composed by non-identical oscillators, then only the CPS between d and r is possible. If further 4)  $\mathbf{F}_i = \mathbf{F}_j, \forall i, j$  (i.e., modular d (r) is composed by identical oscillators), then either the CPS or the global chaotic synchronization (all  $N = N^d + N^r$  nodes of a modular network are in the same complete synchronous state) can occur for certain dynamical parameters. In this letter we call the topological and coupling symmetries the *dynamical symmetry* and study the dynamics of the modular networks composed by identical oscillators to reveal broad synchronized phenomena.

To study the effects of the dynamical symmetry on the stability of the CPS between d and r, considering coupling asymmetry, we give the difference equation:

$$\begin{aligned} \Delta \dot{\mathbf{x}}_i &= \dot{\mathbf{x}}_i^d - \dot{\mathbf{x}}_i^r = \\ &D_i \mathbf{F}_i(\mathbf{x}_i^d) \Delta \mathbf{x}_i + \sum_j g_{ij}^{dd} D_i \mathbf{H}_{ij}(\mathbf{x}_j^d, \mathbf{x}_i^d) \Delta \mathbf{x}_i \\ &+ \sum_j g_{ij}^{rr} D_j \mathbf{H}_{ij}(\mathbf{x}_j^d, \mathbf{x}_i^r) \Delta \mathbf{x}_j + \sum_j \delta_{ij} \mathbf{H}_{ij}(\mathbf{x}_j^d, \mathbf{x}_i^r), \end{aligned} \quad (3)$$

here  $g_{ij}^{dd} - g_{ij}^{rd} - g_{ij}^{rr} = \delta_{ij}$  with  $\delta_{ij}$  being the parameter reflecting the coupling asymmetry. While  $D_i \mathbf{H}_{ij}(\mathbf{x}_j^d, \mathbf{x}_i^d) \times \Delta \mathbf{x}_i = \mathbf{H}_{ij}(\mathbf{x}_j^d, \mathbf{x}_i^d) - \mathbf{H}_{ij}(\mathbf{x}_j^d, \mathbf{x}_i^r)$ , and  $D_i \mathbf{F}_i(\mathbf{x}_i^d) \Delta \mathbf{x}_i = \mathbf{F}_i(\mathbf{x}_i^d) - \mathbf{F}_i(\mathbf{x}_i^r)$ . The  $\sum_{i=1}^{N^d} m_i$  dimension vector  $\Delta \mathbf{x}(t) = (\Delta \mathbf{x}_1(t), \Delta \mathbf{x}_2(t), \dots, \Delta \mathbf{x}_{N^d}(t))^T = 0$  gives the complete CPS. From eqs. (1)–(3) we can calculate the maximal transversal Lyapunov exponent (MTLE)  $\lambda = \lim_{t \rightarrow \infty} \frac{1}{t} \ln |\frac{\Delta \mathbf{x}(t)}{\Delta \mathbf{x}(0)}|$ . The complete CPS is stable for  $\lambda < 0$ , and unstable for  $\lambda > 0$ . It should be noted from the nonhomogeneous differential equation (eq. (3)) that  $\Delta \mathbf{x} = 0$  is the possible solution only for  $\delta_{ij} = 0, \forall i, j$  due to  $\mathbf{H}_{ij}(\mathbf{x}_j^d, \mathbf{x}_i^r) \neq 0$  for general coupled heterogeneous modular networks, i.e., complete CPS can only occur for symmetrical coupling  $g_{ij}^{dd} - g_{ij}^{rd} = g_{ij}^{rr}$ . This result is hold for any complex modular network and will be shown numerically for different modular networks. Since  $\delta \mathbf{x}(t) = \max |\Delta \mathbf{x}(t) / \Delta \mathbf{x}(0)| \sim \exp(\lambda t)$  for  $t \rightarrow \infty$ , the MTLE  $\lambda$  also defines a synchronization time  $\tau_s = |\lambda|^{-1}$  or the speed of synchronization  $\tau_s^{-1} = |\lambda|$ . It is obvious that the complete CPS is faster for more negative MTLE  $\lambda$ . Our following simulation shows that  $\lambda$  strongly depends on both the coupling strength between nodes and the dynamical symmetry of a modular network.

To illustrate the effects of the dynamical symmetry on the CPS and the synchronization speed, we first consider a modular network composed by two interlinked two-dimensional regular lattices with open boundary conditions and  $N^d = N^r = 100$  (see fig. 1b). The nodes are chosen as identical Lorenz oscillators  $\dot{\mathbf{x}} = \mathbf{F}(\mathbf{x}) = [\sigma(y - x), Rx - y - xz, xy - bz]^T$  with  $(\sigma, R, b) = (10, 28, 8/3)$ , and the coupling function as

$$\mathbf{H}(\mathbf{x}_j, \mathbf{x}_i) = \mathbf{E}(\mathbf{x}_j - \mathbf{x}_i) \text{ with } \mathbf{E} = \begin{pmatrix} 0 & 0 & 0 \\ R & 0 & 0 \\ 0 & 0 & 0 \end{pmatrix}. \text{ For symmet-}$$

rical coupling, we set  $g_{ij}^{dd} = g_{ji}^{dd} = \alpha$ , while  $g_{ij}^{rr} = \alpha - \beta$  for  $g_{ij}^{rd} \neq \beta$ , and  $g_{ij}^{rr} = \alpha$  for  $g_{ii}^{rd} = 0$  and  $g_{ij}^{rd} = 0$  (in our calculation the number of  $g_{ij}^{rd} \neq \beta$  is 25, see fig. 1b). The initial conditions of all nodes are chosen from a normal random distribution in the region  $[-10, 10]$ . Figure 2a shows the critical lines of the MTLE  $\lambda(\alpha, \beta) \simeq 0$  (black solid line 1) in  $(\alpha, \beta)$  parameter space. Different regions correspond to different dynamical phenomena, region B (between the black solid line 1 and the vertical dotted line  $\alpha \approx 2.6$ ) corresponds to the complete CPS between modules d and r (see fig. 2b), and region C the global chaotic synchronization, while region D corresponds to the global chaotic synchronization of module d, and region A the unsynchronization of the modular network. Figure 2b shows  $x_i^d(t)$  and  $x_i^r(t), \forall i$ , for different  $(\alpha, \beta, t) = (0.3, 0.3, t), (1.0, 1.0, t), (2.0, 2.0, t)$ . From these three pairs of snapshot of the chaotic pattern (from top to bottom), we see that the chaotic patterns of d and r are identical at the same time, that is, the complete CPS occurs. If  $g_{ij}^{rd} \neq 0$ , and  $g_{ii}^{rd} = \beta, \forall i$  (black nodes in d connect black nodes in r, see fig. 1b), then the complete

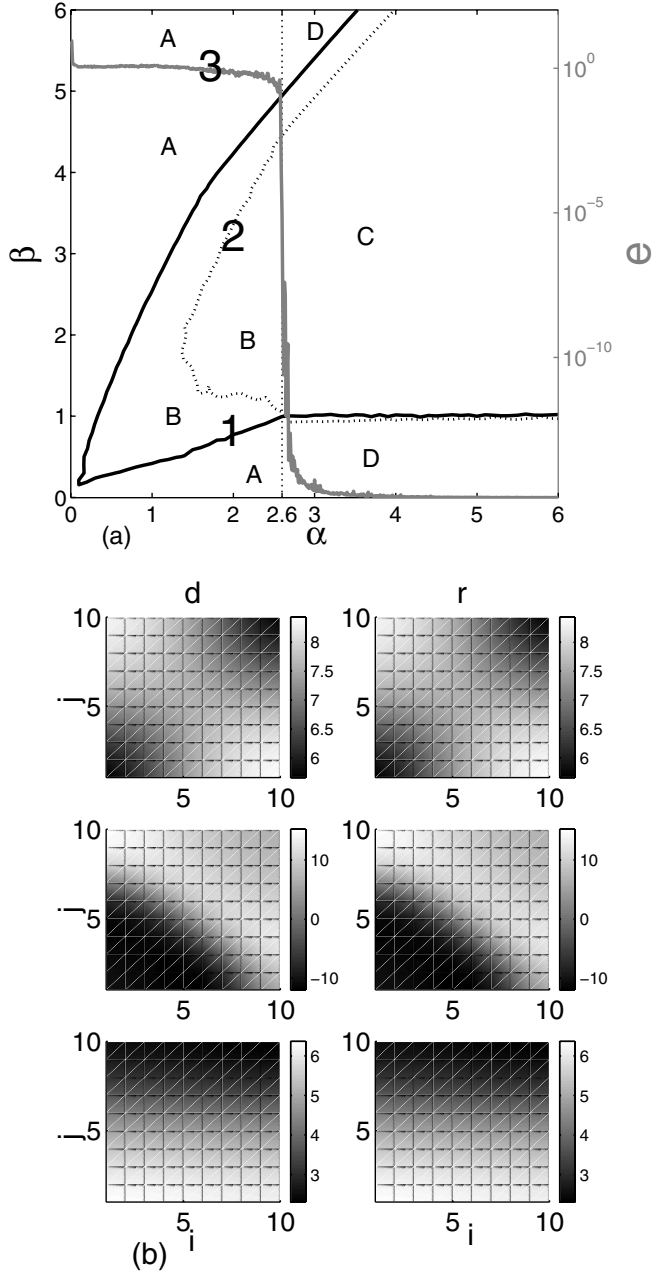


Fig. 2: (a) Stability regions of synchronization of a regular modular network (fig. 1b) obtained by calculating the MTLE  $\lambda(\alpha, \beta)$  for different  $\alpha$ ,  $\beta$ , and  $\beta'$ . The critical lines  $\lambda(\alpha, \beta) \approx 0$  for  $\beta' = \beta$  (line 1) and  $\beta' = \beta + 0.6$  (line 2) divide the parameter space  $(\alpha, \beta)$  into stable and unstable regions. The averaged synchronization error  $e(\alpha) > 10^{-2}$  (line 3) is much larger than  $10^{-15}$  in the complete CPS region B (between line 1 and the vertical dotted line  $\alpha \approx 2.6$ ) and approaches to zero ( $< 10^{-15}$ ) in the global chaotic synchronization region C. A is the unsynchronization region ( $x_i^d \neq x_j^d, x_i^d \neq x_i^r$ ), and D the global chaotic synchronization of module d ( $x_i^d = x_j^d, x_i^d \neq x_i^r$ ), here  $(\sigma, R, b) = (10, 28, 8/3)$ . (b) The chaotic patterns in modules d and r for (from top to bottom)  $(\alpha, \beta, \beta') = (0.3, 0.3, 0.3)$ ,  $(1.0, 1.0, 1.0)$ ,  $(2.0, 2.0, 2.0)$ , and at different time moments. The complete CPS is clearly seen.

CPS can occur for  $0.2 \simeq \alpha_{c1} \leq \alpha < \alpha_{c2} \simeq 2.6$  (in our case) and  $\beta > \beta_c(\alpha)$  (the left region enclosed by the gray solid line 3 in fig. 2a).  $\alpha_{c1}$  can approach zero if all the links  $g_{ii}^{rd} \neq 0$  and  $g_{ij}^{rd} = 0$ . The stability regions for both the complete CPS and the global chaotic synchronization decrease with decreasing the strength  $g_{ij}^{rd}$  and the number of interlinks  $g_{ij}^{rd}$ .

For asymmetrical coupling:  $g_{ij}^{rr} + \delta_{ij} = \alpha - \beta'$  ( $\beta' \neq \beta$ ), the complete CPS disappears and the phase CPS ( $\Delta \mathbf{x} \neq 0$  but the phase difference between node  $i$  in d and node  $i$  in r,  $\forall i$ , is zero) occurs (the region B enclosed by the black dotted line 2 and the vertical dotted line  $\alpha \approx 2.6$  in fig. 2a). The stability regions for both the phase CPS and the global chaotic synchronization increase with decreasing the difference  $|\beta - \beta'|$ , the maximum regions are obtained at  $\beta' = \beta$  (fig. 2a), and the phase CPS becomes the complete CPS. Thus the dynamical symmetry can greatly enhance both the CPS and the global chaotic synchronization.

In order to realize the CPS in a modular network, besides the similar topologies of the modules, the obvious requirements for the dynamical structure of a modular network should be: 1) all the nodes (named drive nodes) in d with zero in-degree should be linked to the nodes in r, 2) any node  $j$  in d with  $g_{ij}^{rd} = 0$  should be driven directly or indirectly by at least one drive node which is linked to r, that is there is (are) flow (flows) from this drive node (nodes) to node  $j$ , 3) there is (are) flow (flows) from d to any node (nodes) in r. With these considerations we study the synchronization speed by calculating the MTLE  $\lambda(\alpha, \beta, \beta')$  for different  $\alpha = g_{ij}^{dd} = g_{ji}^{dd}$ ,  $\beta = g_{ij}^{rd}$ , and  $\beta'$  ( $\alpha - \beta' = g_{ij}^{rr} + \delta_{ij}$ ). The numerical results exhibited in figs. 3a-d show that the stability region enclosed by solid lines for the phase CPS ( $\beta' \neq \beta$ ) decreases with decreasing  $\alpha$  from  $\alpha \simeq 2.6$  since the chaotic states among nodes become more and more different in module d. For  $\alpha \leq 2.6$ , the complete CPS can occur only when  $\beta' = \beta$  corresponding to the dynamical symmetry:  $g_{ij}^{dd} = g_{ij}^{rd} + g_{ij}^{rr}$ . The global chaotic synchronization occurs for  $\alpha \geq 2.6$  and the stability region of it increases with increasing  $\alpha$ . The MTLE  $\lambda$  becomes more and more negative as  $\beta'$  approaches  $\beta$  for any value of  $\alpha$ . The minimum  $\lambda$  is obtained when  $\beta' = \beta$  (see figs. 3a-d). From the behaviors of  $\lambda(\alpha, \beta, \beta')$  in the  $(\alpha, \beta, \beta')$ -space, we see that the synchronization speed  $\tau_s^{-1} = |\lambda(\alpha, \beta, \beta')|$  increases to its maximum value slowly as  $\beta'$  approaches  $\beta$  for larger  $\alpha$ , and abruptly for small  $\alpha$  (see fig. 3l). The difference  $\Delta x_i = x_i^d(t) - x_i^r(t)$  for different  $\alpha$ ,  $\beta$  and  $\beta'$  shown in figs. 3e-k clearly displays the speed-up phenomenon of the synchronization. From  $\Delta x_i$  we can also obtain the synchronization speed  $\tau_s^{-1} \approx \Delta t^{-1}$  ( $\Delta t$  here is the transient time) for different  $\alpha$ ,  $\beta$ , and  $\beta'$ , which have similar behaviors as that of  $\lambda(\alpha, \beta, \beta')$  (see fig. 3l). The spatiotemporal behaviors of the chaotic pattern suggest that the averaged synchronization error  $e(\alpha) = \frac{2}{N^d(N^d-1)} \sum_{i,j} |x_i^d - x_j^d|$  should be much

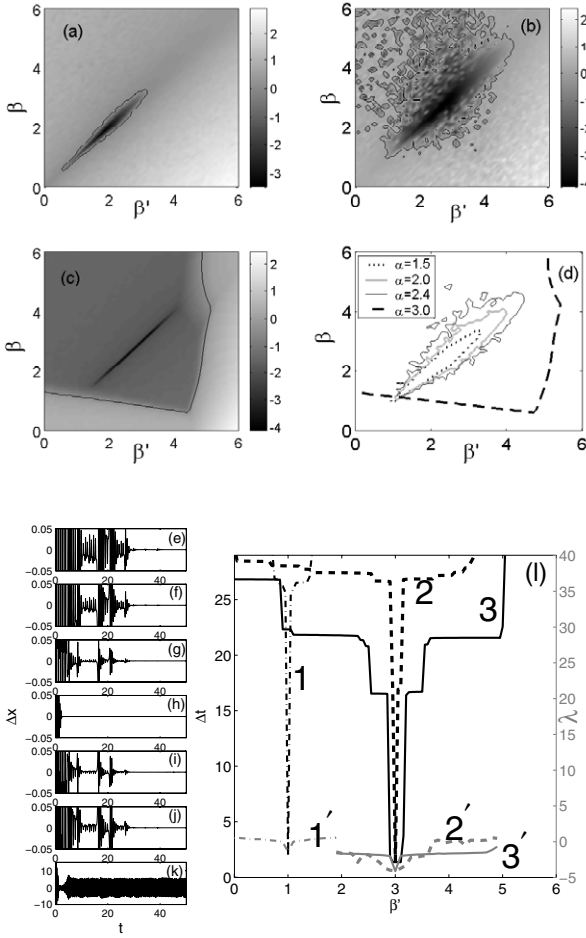


Fig. 3: (a)–(c) The MTLE  $\lambda(\alpha, \beta, \beta')$  of a regular modular network (fig. 1b) for  $\alpha = 1.3$  (a), 2.5 (b), 2.8 (c), and different  $\beta$  and  $\beta'$ . The stable regions enclosed by solid lines increase with increasing  $\alpha$  as shown in (d) and the minimal  $\lambda$ 's are obtained for  $\beta = \beta'$ . The stable regions for  $\beta' \neq \beta$  and  $\alpha \leq 2.6$  are the phase CPS regions. (e)–(k)  $\Delta x(t) = x_i^d(t) - x_i^r(t)$  for  $\alpha = 2.8$ ,  $\beta = 3.0$ , and different  $\beta' = 0.5$  (e), 1.5 (f), 2.7 (g), 3.0 (h), 3.4 (i), 4.5 (j), 5.5 (k). (l)  $\Delta t(\beta')$  (black lines: 1, 2, 3) and the MTLE  $\lambda(\beta')$  (gray lines: 1', 2', 3') for  $(\alpha, \beta) = (1.3, 1.0)$  (lines: 1, 1'),  $(2.5, 3.0)$  (lines: 2, 2'), and  $(2.8, 3.0)$  (lines: 3, 3').  $\beta' = \beta (= 1.0, 3.0)$  gives the minimum  $\lambda$  and the maximum speed of synchronization for different  $\alpha$ .

larger than  $10^{-15}$  (in our case). The numerical results (gray solid line 3 in fig. 2a) show that  $e(\alpha \leq 2.6) > 10^{-2}$  for CPS and  $e(\alpha \geq 2.6) < 10^{-15}$  for global chaotic synchronization.  $\beta'$  must be equal to  $\beta$  for the occurrence of complete CPS if  $e(\alpha \leq 2.6) > 10^{-2}$  (in our case), that is, the dynamical symmetry is the necessary condition for complete CPS if the chaotic states of the nodes in module d are much different from one another ( $e(\alpha) > 10^{-2}$ ). However, the global chaotic synchronization can take place for  $\beta' \neq \beta$  with  $e(\alpha \geq 2.6) < 10^{-15}$ .

It should be noted that the region B still exists, but the region C disappears for lower dynamical symmetry:  $\mathbf{F}_i^d \neq \mathbf{F}_j^d$ ,  $\mathbf{F}_i^r \neq \mathbf{F}_j^r$ , but  $\mathbf{F}_i^d = \mathbf{F}_i^r$ . We have numerically calculated

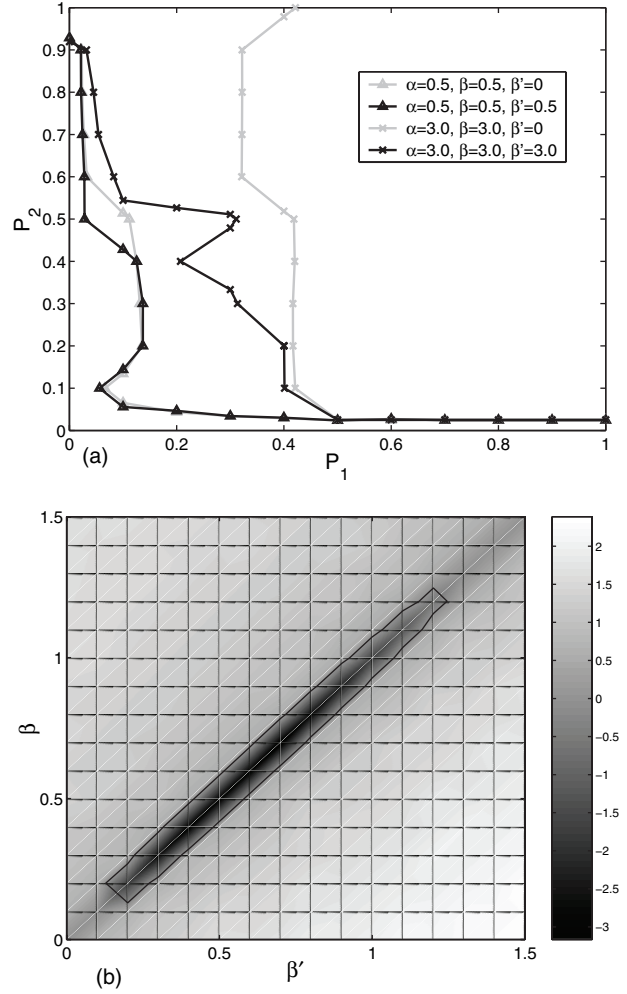


Fig. 4: The MTLE  $\lambda$  of the random modular networks (fig. 1c) (averaged over 10 realizations). (a) The MTLE  $\lambda(P_1, P_2)$  for different  $\alpha$ ,  $\beta$ , and  $\beta'$  (for details, see the text). (b) The MTLE  $\lambda$  for  $P_1 = 0.08$ ,  $P_2 = 0.5$ ,  $\alpha = 0.5$ , and different  $\beta$  and  $\beta'$ , which shows that the complete CPS occurs for  $\beta' = \beta$ , and the phase CPS occurs for  $\beta' \neq \beta$  (region enclosed by the black solid line).

this result in a heterogeneous modular network composed by non-identical Lorenz oscillators.

As another example to further show the generality of the relations between the dynamical symmetry and the synchronization, we consider a modular network composed of two randomly intralinked modules with the intralinked probability  $P_2$  which are randomly interlinked with the interlinked probability  $P_1$  (see fig. 1c). In generating the random modular networks the relations  $g_{ij}^{dd} - g_{ij}^{rd} - g_{ij}^{rr} = \delta_{ij}$  is kept, and the identical Lorenz oscillators with  $(\sigma, R, b) = (10, 28, 8/3)$  and  $N^d = N^r = 50$  are used. The MTLE  $\lambda(P_1, P_2)$ 's for different  $P_1$ ,  $P_2$ ,  $\alpha$ ,  $\beta$ , and  $\beta'$  are shown in fig. 4, which are obtained from the average over 10 realizations of the modular networks. For the same  $\alpha$  and  $\beta$ , the critical lines  $\lambda(P_1, P_2) \simeq 0$  for  $\beta' = 0$  (gray lines) and  $\beta' = \beta$  (black lines) are illustrated in fig. 4a. For the same  $\alpha$ , the right region of the gray line is the stability region for global chaotic synchronization, and the

left region of the black line is for the unsynchronization, while the region between the black and the gray lines is for the complete CPS. The complete CPS region disappears and a small region for the phase CPS occurs for  $\beta' \neq \beta$  as shown in fig. 4b. Because more links between modules d and r are required for CPS as  $\alpha$  is increased, so that the stability region for complete CPS in  $(P_1, P_2)$  parameter space increases with increasing  $\alpha$ . We have studied the bidirectionally coupled modular networks with linear and ring structures and obtained the similar results as discussed above.

In summary, we have shown that the dynamical symmetry between modules are the requirements for complete CPS in modular networks. Since nodes  $i \in d$  and  $i \in r, \forall i$ , are identical, the condition for complete CPS can be equally stated as: the same and identical inputs of nodes  $i$  in d and  $i$  in r are required for complete CPS, that is,  $\sum_j g_{ij}^{dd} \mathbf{H}(\mathbf{x}_j^d, \mathbf{x}_i^d) = \sum_j g_{ij}^{rd} \mathbf{H}(\mathbf{x}_j^d, \mathbf{x}_i^r) + \sum_j g_{ij}^{rr} \mathbf{H}(\mathbf{x}_j^r, \mathbf{x}_i^r)$ . In the complete chaotic pattern synchronous state:  $\mathbf{x}_i^d(t) = \mathbf{x}_i^r(t)$  and  $\mathbf{x}_j^d(t) = \mathbf{x}_j^r(t), \forall i$ , which yield  $\mathbf{H}(\mathbf{x}_j^d, \mathbf{x}_i^d) = \mathbf{H}(\mathbf{x}_j^d, \mathbf{x}_i^r) = \mathbf{H}(\mathbf{x}_j^r, \mathbf{x}_i^r)$  and  $g_{ij}^{dd} = g_{ij}^{rd} + g_{ij}^{rr}$ . This *micro-condition* is crucial for complete CPS with high speed in modular complex networks. The dynamical symmetry is closely related to the groupoid, which was used to discuss the network dynamics [13]. It should be stressed that the dynamical symmetry is only a necessary condition for synchrony, which is not a sufficient condition, because the network synchronization is strongly dependent on the coupling schemes, coupling strength and the network size. For example, the synchrony cannot exist in larger enough square lattices with nearest-neighbor coupling between Lorenz oscillators even though the networks have groupoid structure. Our results may have potential applications in complex networks and communication technologies, where the CPS and high-speed information flow are important, for example, we can use complete CPS to decode information in chaos communication where complex modular networks are used to generate hyperchaos to mask information [14].

\*\*\*

We acknowledge the support from the NSF of Jiangsu Province (No. BK2005062). HJW is supported by a grant from Nanjing Xiaozhuang University and the QingLan Project of Jiangsu Province (No. 4074007). GXQ is supported by the Helmholtz-CSC Fellowship 2007.

## REFERENCES

- [1] BLASIUS B., HUPPERT A. and STONE L., *Nature (London)*, **399** (1999) 354.
- [2] FRIES P., REYNOLDS J. H., RORIE A. E. and DESIMONE R., *Science*, **291** (2001) 1560; SEIDENBECHER T., LAXMI T. RAO, STORK O. and PAPE HANS-CHRISTIAN, *Science*, **301** (2003) 846; HASSON U., NIR Y., LEVY I., FUHRMANN G. and MALACH R., *Science*, **303** (2004) 1634; BUZSÁKI G. and DRAGUHN A., *Science*, **304** (2004) 1926.
- [3] KISS I. Z., ZHAI Y. and HUDSON J. L., *Science*, **296** (2002) 1676; *Phys. Rev. Lett.*, **88** (2002) 238301.
- [4] ROGERS E. A., KALRA R., SCHROLL R. D., UCHIDA A., LATHROP D. P. and ROY R., *Phys. Rev. Lett.*, **93** (2004) 084101.
- [5] FUKUYAMA T., KOZAKOV R., TESTRICH H. and WILKE C., *Phys. Rev. Lett.*, **96** (2006) 024101.
- [6] PECORA L. M., *Phys. Rev. E*, **58** (347) 1998; HE S. H., HUANG H. B., ZHANG X., LIU Z. X., XU D. S. and SHEN C. K., *Phys. Rev. E*, **74** (2006) 057203.
- [7] ZHOU C., MOTTER A. E. and KURTHS J., *Phys. Rev. Lett.*, **96** (2006) 034101.
- [8] BARAHONA M. and PECORA L. M., *Phys. Rev. Lett.*, **89** (2002) 054101.
- [9] HWANG D.-U., CHAVEZ M., AMANN A. and BOCCALETTI S., *Phys. Rev. Lett.*, **94** (2005) 138701; CHAVEZ M., HWANG D.-U., AMANN A., HENTSCHEL H. G. E. and BOCCALETTI S., *Phys. Rev. Lett.*, **94** (2005) 218701; ZHOU C. and KURTHS J., *Phys. Rev. Lett.*, **96** (2006) 164102.
- [10] HUANG L., PARK K., LAI Y.-C., YANG L. and YANG K., *Phys. Rev. Lett.*, **97** (2006) 164101.
- [11] SUR M. and RUBENSTEIN J. L. R., *Science*, **310** (2005) 805; OH E., RHO K., HONG H. and KAHNG B., *Phys. Rev. E*, **72** (2005) 047101; JALAN S. and AMRITKAR R. E., *Phys. Rev. Lett.*, **90** (2003) 014101; MANRUBIA S. C. and MIKHAILOV A. S., *Phys. Rev. E*, **60** (1999) 1579; ZHOU C., ZEMANOVÁ L., ZAMORA G., HILGETAG C. C. and KURTHS J., *Phys. Rev. Lett.*, **97** (2006) 238103; ARENAS A., DÍAZ-GUILERA A. and PÉREZ-VICENTE C. J., *Phys. Rev. Lett.*, **96** (2006) 114102.
- [12] MILO R., SHEN-ORR S., ITZKOVITZ S., KASHTA N. N., CHKLOVSKII D. and ALON U., *Science*, **298** (2002) 824; RAVASZ E., SOMERA A. L., MONGRU D. A., OLTVAI Z. N. and BARABÁSI A.-L., *Science*, **297** (2002) 1551.
- [13] IAN STEWART, *Nature (London)*, **427** (2004) 601.
- [14] ZHOU J., HUANG H. B., QI G. X., YANG P. and XIE X., *Phys. Lett. A*, **335** (2005) 191.